CHANGES IN PHYSICAL PROPERTIES OF YELLOW BIRCH BELOW AND ABOVE THE FIBER SATURATION POINT

Giana Almeida†
Ph.D. Candidate

and

Roger E. Hernández†
Professor
Département des Sciences du Bois et de la Forêt
Université Laval
Québec, Canada, G1K 7P4

(Received December 2004)

ABSTRACT

Two experimental techniques were used to perform moisture sorption tests at 25ºC on specimens of yellow birch sapwood. The first used saturated salt solutions (from 33% to 90% relative humidity), and the second used the pressure membrane method (above 96% relative humidity). These sorption tests were combined with dimensional measurements and perpendicular-to-the-grain tangential compression tests. Results showed that at equilibrium moisture content, radial, tangential, and volumetric shrinkage, as well as changes in transverse strength, occur above the fiber saturation point. This behavior can be explained by the effect of hysteresis at saturation on wood properties. This hysteresis indicates that loss of bound water takes place in the presence of liquid water, which contradicts the concept of FSP. The initial equilibrium moisture content at which bound water is removed from yellow birch was about 41%.

Keywords: Equilibrium moisture content, desorption, wood strength, compliance coefficient, shrinkage.

INTRODUCTION AND BACKGROUND

The fiber saturation point (FSP) is an important feature of wood. This property was initially defined by Tiemann (1906) as the moisture content (MC) at which the cell walls are saturated with bound water with no free water in the cell cavities. It is normally assumed that the FSP is the MC below which the physical and mechanical properties of wood begin to change as a function of MC (USDA 1974; Siau 1984). The FSP is hence used in models to adjust the mechanical properties of wood as a function of its MC (Bodig and Jayne 1982), as well as in wood shrinkage and density adjustment models (Siau 1984; Skaar 1988).

However, some results reported in the literature show that this assumption may not be realistic. Stevens (1963) found that shrinkage in beech begins to take place above the FSP. This researcher suggested a MC gradient effect for explaining this behavior, but this hypothesis appears incompatible with the fact that shrinkage values reported in this study were measured at equilibrium moisture content (EMC). Goulet and Hernández (1991) reported a large hysteresis effect on the EMC and on the perpendicular-to-the-grain tangential tension strength of sugar maple wood at high relative humidities (RH). The difference for the tangential tension strength between adsorption and desorption states was 20% at 26% EMC. This effect was attributed to the hysteresis at saturation phenomenon, which affected the wood moisture sorption above 63% RH (Hernández 1983). This hysteresis implies that during desorption the loss of bound water begins before all liquid water has been removed from the wood.

† Member of SWST

Wood and Fiber Science, 38(1), 2006, pp. 74 – 83

Even though desorption curves had 26% EMC as an upper limit, Goulet and Hernández (1991) predicted that the effect of MC on sugar maple wood properties could be extended beyond the FSP, estimated to be 31% MC. A later study focusing on high humidities (above 90% RH) was hence conducted for the same wood (Hernández and Bizoň 1994). The results demonstrated that at the EMC, changes in transverse and volumetric shrinkage, as well as changes in transverse strength, occur above the nominal FSP. The initial EMC at which bound water is removed from sugar maple wood was about 42.5%. This occurs even with the presence of liquid water within the wood structure. These results were outlined later by Siau (1995) when describing the fiber saturation point. However, the effect of hysteresis at saturation on wood properties has so far been reported for only one species. More research on other wood species is needed in order to further enlarge these conclusions.

The main objective of this investigation was therefore to study the effect of EMC on wood properties of yellow birch below and above cell-wall saturation. Two moisture sorption techniques using saturated salt solutions (between 33% and 90% RH) and the pressure membrane method (above 96% RH) were applied to large samples at 25ºC. These sorption tests were combined with shrinkage measurements as well as perpendicular-to-the-grain tangential compression tests.

MATERIAL AND METHODS

Experiments were carried out with yellow birch (*Betula alleghaniensis* Britton) wood. Specimens for the pure perpendicular-to-the-grain tangential compression tests were cut with a cross-section of 20 mm (R) by 20 mm (L) and a height of 60 mm (T). The choice of dimensions was limited by the matching techniques used and by the length of the sorption experiments. A length-to-width ratio of 3 was used to preclude buckling during the tangential compression test (Bodig and Jayne 1982) and to limit the effect due to the growth ring curvature.

Sixty green defect-free flatsawn pieces taken from three trees were carefully selected and stored in a conditioning room at 20°C and 60% RH. After conditioning, pieces were cut to obtain boards 20 mm (R) by 60 mm (T) and 500 mm (L). The twenty best boards were selected based on a good growth ring orientation (to limit its curvature), growth ring uniformity, and by eliminating the lighter and heavier boards, a low wood density variation among boards was assured. Twelve adjacent specimens were chosen from each board to investigate twelve moisture conditions. This longitudinal matching yielded twelve comparable groups of twenty specimens each. The test material was all sapwood with an average basic wood density (oven-dry mass to green volume) of 533 kg/m^3, with a coefficient of variation of 4%.

Experiments

The experiments consisted of a series of moisture sorption tests associated with shrinkage and mechanical tests. Wood specimens were mechanically tested as soon as the desired EMC was reached. There were ten points in desorption and one in adsorption (Table 1). Prior to the desorption tests, specimens were saturated in three steps until their full moisture content was reached. This was done in order to avoid internal defects caused by a rapid moisture adsorption (Naderi and Hernández 1997). Thus, specimens were conditioned over a KCl saturated salt solution for 30 days, then over distilled water for at least 60 days, and finally they were immersed in distilled water until full saturation by cycles of vacuum and pressure. At this state, their full saturated masses were measured to the nearest 0.001 g with a digital balance, and dimensions in all principal directions were taken to the nearest 0.001 mm with a digital micrometer. The group to be conditioned in adsorption over distilled water was kept at 20ºC and 60% RH prior to the adsorption test.

The sorption experiments required two experimental techniques. The first technique involved the use of saturated salt solutions. In the second one, specimens were conditioned following a pressure membrane procedure. The first technique was carried out at between 33% and

TABLE 1. *Characteristics of the moisture sorption conditions used in these experiments and results of the equilibrium moisture content (EMC).*

State of sorption	Chemical or saturated salt solution	Nominal relative humidity (%)	Water potential (Jkg^{-1})	EMC (%)	Radius of curvature of the air-water meniscus (μm)[1]
		Full saturation under distilled water			
Saturation	H_2O	100	0	118.18 (4.33)[2]	∞
		Equilibrium under a pressure membrane at 25°C			
Desorption	—	99.927	−100	82.70 (6.20)	1.440
Desorption	—	99.782	−300	69.20 (12.41)	0.480
Desorption	—	99.492	−700	41.18 (3.61)	0.206
Desorption	—	98.557	−2 000	38.58 (3.01)	0.072
Desorption	—	96.431	−5 000	34.62 (5.87)	0.029
		Equilibrium over saturated salt solutions at 25°C			
Adsorption	H_2O	≈100	—	34.56 (3.65)	—
Desorption	$ZnSO_4$	90	−14 495	23.66 (0.99)	—
Desorption	KCl	86	−20 750	21.40 (1.39)	—
Desorption	NaCl	76	−37 756	17.51 (0.87)	—
Desorption	NaBr	58	−74 941	12.36 (1.11)	—
Desorption	$MgCl_2$	33	−152 526	7.46 (0.50)	—

[1] According to the capillary pressure equation (Eq. 2). Under about 92% RH, equation is not applicable.
[2] Values between parentheses represent the coefficient of variation of EMC based on 20 specimens.

90% RH, as well as over distilled water, using sorption vats described in detail by Goulet (1968). These vats provide a temperature control of ± 0.01°C during extended periods, thus allowing for precise RH control in the various desiccators serving as small sorption chambers. For each point of sorption, one desiccator containing twenty samples was used. All five desorption conditions were over saturated salt solutions in a single step procedure. The adsorption test over distilled water involved an intermediate step of 30 days over a saturated KCl solution (two step procedure). The time of conditioning varied between 133 days (adsorption at ≈ 100% RH) and 419 days (desorption at 90% RH). For each point of sorption, control specimens were weighted periodically, without being removed from the desiccator. It was assumed that the EMC was reached when the loss (desorption) or gain (adsorption) in MC was at least less than 0.003% MC per day.

The pressure membrane procedure was used to determine five additional points of desorption between 96.431% and 99.927% RH (Table 1). This technique is suitable for this humidity range and has been used by many researchers before (Robertson 1965; Stone and Scallan 1967; Griffin 1977; Fortin 1979; Hernández and Bizoň 1994). The procedure introduces the concept of water potential (ψ or WP), which is derived from classical thermodynamics and is defined as the difference between the specific Gibbs free energies of water in the state under study and in a standard reference state (Siau 1984, 1995). The

reference state generally used is a hypothetical pool of pure free water at atmospheric pressure, at a given elevation, and at the same temperature as that of the water in the porous material (Fortin 1979; Cloutier and Fortin 1991). The water potential is considered as the driving force for the movement of moisture within wood and is normally expressed in terms of energy per unit mass in Jkg^{-1}. Relationships between water potential (ψ) and RH are shown in Table 1. The water potential of moist air may be calculated from Eq. 1.

$$\psi = \frac{\rho_\omega RT \ln h}{0.018} \quad (1)$$

where: $\rho\omega$ is the normal density of water; R is the gas constant (8.31 J mol^{-1} K^{-1}); T is the absolute temperature (K); h is the relative vapor pressure.

The radius of curvature of the air-water meniscus (r) is also presented in Table 1. This radius can be calculated because of the relationship existing between the pressure applied on the sample side of a pressure membrane apparatus and the capillary structure of wood (Eq. 2):

$$r = \frac{-2\gamma \cos\theta}{\psi} \quad (2)$$

where: γ is the surface tension of water (0.072 N m^{-1} at 25ºC); θ is the contact angle between the liquid and the surface of the capillary (0º).

For each point of longitudinal desorption, twenty fully saturated specimens were placed into the pressure extractor on a saturated cellulose acetate membrane. A detailed description of the apparatus is given by Cloutier and Fortin (1991). A saturated clay layer about 2 mm thick was placed on the membrane in order to ensure permanent hydraulic contact with the specimens (Fortin 1979). Pressure was then gradually applied until the required level was reached. Flow of water was collected in a burette. EMC was considered as reached when outflow became negligible (no outflow during seven successive days). These experiments required between eleven and twenty-two days of desorption, depending on the ψ considered.

As soon as each sorption test was completed, the sample mass was measured to the nearest 0.001g. Dimensions in all principal directions were taken to the nearest 0.001 mm with a micrometer. Tangential compression tests were immediately carried out on a Riehle machine equipped with an appropriate load cell. The strain was measured over a span of 40 mm on the central part of the specimen, using a two-side clip gauge provided with a Sangamo DG 1.0 linear displacement sensor (LVDT). In addition, the entire deformation of the specimen was measured by the displacement of the cross-head, using another Sangamo LVDT. Hygrothermal changes during all mechanical tests were controlled by wrapping the specimen in cotton that had been previously conditioned above the same humidity conditions as the wood. As per Sliker (1978), the cross-head speed was adjusted in order to ensure a similar strain rate for all moisture conditions. In the elastic range, this strain rate was 0.40 mm/mm/min.

In addition to the sorption experiments, a group of samples that had been fully saturated with distilled water was mechanically tested. This was done to compare the properties measured under this condition with those evaluated from the group conditioned over distilled water.

The test results were used to calculate the compliance coefficient in the tangential direction (s_{33}) of the wood. The reciprocal of this parameter is Young's modulus. Strain-stress curves were plotted using consecutive strain-stress readings recorded by a data acquisition system. Stress at the proportional limit was defined as where the recorded strain differed by 1% of that estimated by a linear regression analysis using all lower strain readings obtained within the elastic range of the curve. The cross-sectional area used for the calculations was that measured at the time of testing. The differences in dimensions of specimens after full moisture saturation and before the mechanical test were used to estimate the partial percent shrinkage in the tangential (β_{TH}) and radial (β_{RH}) direction of the wood. Volumetric shrinkage was estimated to be the summation of these two directional shrinkages ($\beta_{TH} + \beta_{RH} - \beta_{TH} . \beta_{RH}$). The mass of the specimens just before the mechani-

cal test and their mass measured after oven-drying were used to calculate the EMC, expressed as a percentage of oven-dry mass.

RESULTS AND DISCUSSION

Wood hygroscopicity

The mean and coefficient of variation of EMC are shown in Table 1. The coefficient of variation of EMC values generally increased as relative humidity increased. Sorption at high humidities is mainly affected by capillary forces. Thus, the higher variation in EMC at high humidities could be principally due to variations in the capillary structure among the twenty samples used.

The relationship between water potential and EMC for yellow birch wood is given in Fig. 1. Previous results obtained for sugar maple wood (Hernández and Bizoň 1994) are also added for comparative purposes. This figure displays only the desorption curve obtained by using either the pressure membrane or the saturated salt solution methods. In all cases, the standard errors of the EMC data do not exceed the symbol size shown. An excellent continuity is apparent between the results obtained by both sorption methods. This confirms the suitability of the pressure membrane method for determining EMC in wood under high relative humidity conditions, which is consistent with numerous earlier reports (Stone and Scallan 1967; Cloutier and Fortin 1991; Hernández and Bizoň 1994).

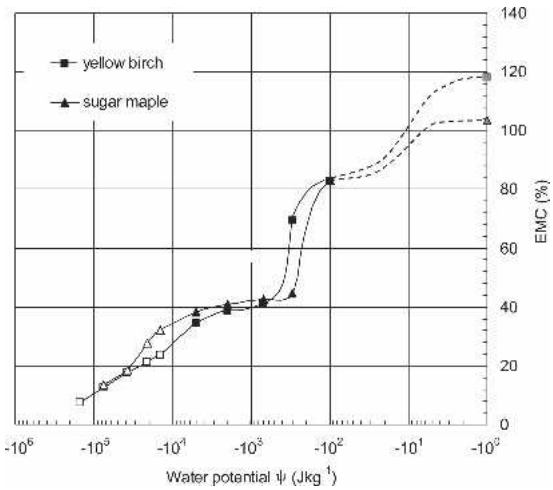

FIG. 1. Equilibrium moisture content-water potential relationship of yellow birch and sugar maple sapwoods along the boundary desorption curve for longitudinal desorption at 25°C (yellow birch) and 20–21°C (sugar maple, from Hernández and Bizoň 1994). The gray symbols at -10^0 Jkg^{-1} WP represent full saturation under distilled water; black symbols are the values obtained by the pressure membrane method, and white symbols are the values obtained under the saturated salt solution method.

In this study, the desorption was carried out beginning from the fully saturated state, and the curve obtained corresponds to the maximum EMC expected for each humidity condition. The term boundary desorption curve is therefore used to describe this feature. Any desorption curve obtained from a lower initial MC would be located below this boundary desorption curve.

The region between 96% and 100% RH is greatly expanded when using the water potential concept to represent sorption isotherms. This region is very important when studying the wood-water interactions given that it is mainly controlled by the capillary forces and consequently by the micro-structure of wood species. Since wood is a porous material, an important effect that has to be considered in the interpretation of Fig. 1 is the "ink-bottle effect." The capillary system of wood consists of cavities interconnected by narrow channels. The variation in dimensions between the different types of cavities connected in series suggests that desorption tends to be governed by a lower water potential, which is determined by the narrower sections of the pores. In contrast, adsorption tends to be governed by a higher water potential, which depends on the larger sections of the pores. Thus, the desorption isotherm will depend on the size of channels connecting the lumina, whereas the adsorption isotherm will depend on the size of these lumina (Fortin 1979).

Figure 1 shows that water drainage between full saturation and -100 Jkg^{-1} WP was about 35.5% MC. In terms of mass units, this corresponds to a loss of 5.188 g of liquid water. This water would have occupied a volume of about 21.4% within the wood specimen (mean volume of the specimen at 12% EMC was 24.2 cm^3).

From the discussion above, it appears that this water would have been removed from the larger capillaries, especially the vessel lumina. According to Panshin and de Zeeuw (1980), the proportion of vessel lumina in yellow birch is 21.4% of the total volume. Table 1 indicates that at -100 Jkg^{-1}, WP capillaries with radius larger than 1.44 μm are already empty. Since the radius of vessel elements in birch species is between 30 and 80 μm (Brown et al. 1949), it is apparent that all vessel elements were empty at this stage of desorption.

The boundary desorption curve of yellow birch changes sharply between -100 Jkg^{-1} and -700 Jkg^{-1} WP, and plateaus between -700 Jkg^{-1} and $-2\,000$ Jkg^{-1} WP (Fig. 1). Changes in EMC for sugar maple in this region of WP were more abrupt, and the plateau corresponded instead to WPs between -300 Jkg^{-1} and $-2\,000$ Jkg^{-1}. This implies that yellow birch presents the least capillaries with a radius larger than 0.48 μm (-300 Jkg^{-1}) compared to sugar maple (Table 1). The difference in EMC between the two species at -300 Jkg^{-1} WP was about 26%. On the other hand, these species exhibit a similar volume of capillaries with a radius larger than 0.21 μm (-700 Jkg^{-1} WP). The results indicate that complete drainage of the fiber cavities would be accomplished at -300 Jkg^{-1} WP for sugar maple and at -700 Jkg^{-1} WP for yellow birch wood. This drainage would depend on the size of openings between the pit membrane strands connecting fibers. This means that the mean radius of these openings could be larger for sugar maple (0.48 μm) than for yellow birch wood (0.21 μm). Observations undertaken on scanning electronic microscopy (SEM) images (not shown) have corroborated such findings.

The plateau observed between -700 Jkg^{-1} and $-2\,000$ Jkg^{-1} WP for yellow birch indicates that openings controlling the retention and flow of water are scarce within these WP values. The water remaining in wood would be localized in capillaries having a radius equal to or smaller than about 0.072 μm (Table 1). The plateau shown would correspond to the transition between the drainage of the fiber cavities and the drainage of cell walls, and longitudinal and ray parenchyma lumina. As discussed later, an important part of the liquid water remaining below -700 Jkg^{-1} WP in yellow birch could be entrapped in the parenchyma cells as noted by Hart (1984).

For softwood species, Fortin (1979) and Tremblay et al. (1996) observed a drainage curve with no intermediate plateau. Aspen wood presented this feature but at higher WPs values (-25 to -100 Jkg^{-1}) than yellow birch and sugar maple (Cloutier and Fortin 1991). Such results confirm that at high humidities, the EMC-WP relationship is highly dependent on species.

Values of EMC for yellow birch in the range of $-2\,000$ Jkg^{-1} and $-20\,750$ Jkg^{-1} WPs were lower than those reported previously for sugar maple wood (Fig. 1). This suggests that sugar maple could have more blocked cavities restraining the drainage of the remaining liquid water at these levels of WP. An analysis of SEM images (not shown) indicated that pit rays in sugar maple were very scarce.

The boundary desorption curves of yellow birch and sugar maple almost join below 76% RH (Fig. 1). This was expected given that desorption of liquid water at this level of RH is almost achieved. More precisely, Hernández (1983) reported that loss of liquid water for sugar maple will be accomplished at about 63% RH, which corresponds to nearly 14% EMC. It is recognized that bound water desorption is quite similar among different temperate neutral woods.

The FSP value of 34.6% for yellow birch obtained in adsorption over distilled water (Table 1) was higher than the expected one estimated by the volumetric shrinkage intersection point method (Fig. 2). The FSP determined by this method (moisture content at which the extended linear portion of shrinkage-moisture curve intersects the line of zero shrinkage) was about 29.2%. For this estimation, only volumetric shrinkage values obtained between 33% and 76% RH were used. This was done because of the nonlinearity of the shrinkage-moisture curve at low moisture contents (Kelsey 1956) and the effect of the hysteresis at saturation on shrinkage at high moisture contents (Hernández and Bizoň

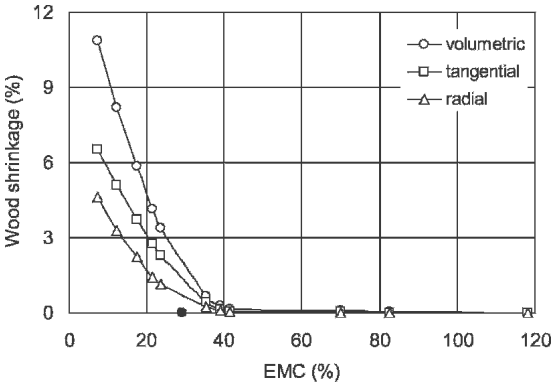

FIG. 2. Shrinkage of yellow birch sapwood as a function of the EMC at 25°C. The symbol • represents the FSP estimated by the volumetric shrinkage intersection method (standard errors are shown only when they exceed the symbol size).

1994). It is clear that the FSP value determined by adsorption over distilled water was overestimated due to a water condensation occurring in the cell cavities and intercellular spaces. Hernández (2005) has indicated that the adsorption test over distilled water for determining FSP is not applicable for all wood species. Condensation occurred in woods exhibiting a large range of densities and micro-anatomical structures. Consequently, the FSP value of yellow birch estimated by the volumetric shrinkage intersection point method will be used in the discussion that follows.

Wood shrinkage—EMC relationships

The relationships between the EMC and the radial, tangential and volumetric shrinkages of yellow birch are shown in Fig. 2. This figure indicates that radial, tangential, and volumetric shrinkages begin at about 41% EMC, which corresponds to -700 Jkg^{-1} WP. In this study, the amount of bound water or actual FSP for yellow birch was estimated to be 29.2%, which indicates that shrinkage started before the FSP was reached. This means that, even at equilibrium, loss of bound water within the cell walls provokes shrinkage of wood before all liquid water has evaporated. For sugar maple wood, Hernández and Bizoň (1994) stated that shrinkage began at 42.5% EMC even though the FSP of this species is 31%. Stevens (1963) also noted that shrinkage begun well before the FSP for beech wood.

This implies that about 12% MC in liquid form is still retained in the wood when shrinkage of yellow birch starts taking place at -700 Jkg^{-1} WP (41.2% – 29.2% EMC). In terms of mass units, this corresponds to 1.7 g of liquid water that would have occupied a volume of about 7% within the wood specimen (mean volume of the specimens at 12% EMC was 24.2 cm^3). Given the level of WP concerned, this water could be entrapped in wood cells interconnected by the smallest capillaries or channels. Hernández and Bizoň (1994) stated that this would correspond to the openings in the membranes of the simple pit pairs located between radial parenchyma cells. The presence of liquid water principally in the rays seems feasible, given that these wood elements are considered as the least permeable flow path in hardwoods (Siau 1984, 1995). Such elements should be so impermeable that loss of bound water by diffusion starts taking place in the other more permeable wood tissues. Wheeler (1982) noted that the parenchyma-parenchyma pit membranes are thicker than both the intervessel pit membranes and the fiber-fiber pit membranes, and consequently are less efficient pathways for liquid flow. This entrapped water could in fact principally fill the 10.8% volume of ray tissue reported for yellow birch by Panshin and de Zeeuw (1980). The entrapment of liquid water in ray tissue reported by Hart (1984) for hickory and oak adds further support to this hypothesis. Menon et al. (1987) studied the water location during the drying of Douglas-fir and western red cedar using proton magnetic resonance technique. Under unequilibrated conditions, liquid water remained in the ray and tracheid compartments when bound water begins to leave the cell wall at 31% MC. The liquid water was all lost when the MC reached values as low as 9%. According to Skaar (1988), the presence of water-soluble materials in the cavities of parenchyma cells may reduce the humidity at which moisture may condense. Detailed studies

of wood structure are needed before the location of entrapped liquid water can be known.

Tangential compression strength—EMC relationships

The relationship between EMC and the compliance coefficient (s_{33}) for yellow birch are shown in Fig. 3. This figure displays the compliance coefficient measured over the central part of the sample (40 mm), as well as the coefficient estimated over its entire length.

A comparison between the curves obtained in the central part and over the entire length shows that there is a heterogeneous distribution of the strain inside the wood specimen. Entire compliance coefficient s_{33} was on average 30% higher than the median compliance coefficient. This behavior has already been observed in other studies (Hernández 1993; Hernández and Bizoň 1994). The difference in strains can be partially attributed to the stress concentrations introduced by lateral strains near the end surfaces of sample, which are in contact with the testing machine (Bodig and Jayne 1982). Standard test methods specify the use of the central part of the specimen for measurement of deformation.

The effect of the hysteresis at saturation on the tangential compliance coefficient of yellow birch can be observed in Fig. 3. This is apparent when comparing the s_{33} obtained at the FSP (29.2%) with the one from the boundary desorption curve at a similar EMC. The difference between the s_{33} values obtained at 29.2% EMC was 14% for both types of strains evaluated. However, the compliance coefficient values of yellow birch (Fig. 3) showed a greater variation at high EMC values. As a result, the initial MC at which the s_{33} property starts to change could not be determined.

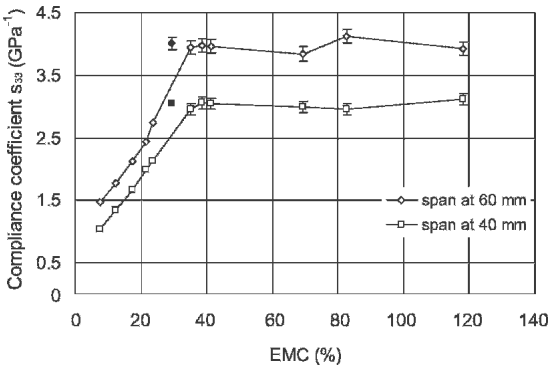

FIG. 3. Compliance coefficients s_{33} in tangential compression of yellow birch sapwood as a function of the EMC. The symbols ♦ and ■ represent the FSP estimated by the volumetric shrinkage intersection method (standard errors are shown only when they exceed the symbol size).

For sugar maple wood, Hernández and Bizoň (1994) reported a difference of about 10% between the compliance coefficient obtained at the FSP (31.1%) and that measured at the maximum MC (full saturation). This difference was attributed to the saturation treatment used to attain the maximum MC, where samples of 14% EMC were directly immersed in distilled water. In the present study, the saturation treatment was performed in three steps, which resulted in statistically equal values at the FSP and at the maximum MC. This finding shows that a mild saturation effectively avoids internal defects in wood samples and has to be considered in future studies as suggested by Naderi and Hernández (1997).

General discussion

As noted for shrinkage, gain in tangential strength of yellow birch started before the FSP was reached (Fig. 3), as a result of the loss of bound water in presence of liquid water. Hernández and Bizoň (1994) observed that, in sugar maple, such changes in physical properties started at 42.5% EMC. In our case, shrinkage results showed that changes in wood properties started at nearly 41% EMC for yellow birch. This EMC would represent the practical FSP proposed by Siau (1984) as that MC corresponding to abrupt changes in physical properties of wood. However, this value does not correspond to any abrupt transition from bound water to liquid water as currently stated. These findings need to be incorporated into the models that are used to adjust the mechanical properties of clear wood as a function of its MC, together with wood shrinkage and density adjustment models.

Use of the terms "green" or "water-saturated" for wood having an MC above but approaching the nominal FSP should also be reconsidered. The results of this study also show that during desorption a region exists where the loss of bound water takes place in the presence of liquid water. The range of EMC of this region will depend on the size distribution of wood capillaries and, as a result, this will vary among wood species.

SUMMARY AND CONCLUSIONS

Moisture adsorption and desorption experiments were performed in specimens of yellow birch sapwood at 25ºC. Special attention was paid to the fiber saturation zone. Once equilibrium was reached, shrinkage measurements and tangential compression tests were undertaken. The results of these tests lead to the following main conclusions:

1. At equilibrium, the radial, tangential shrinkage and, consequently, the volumetric shrinkage begin well above the actual fiber saturation point.
2. At equilibrium, the moisture content affects the tangential compliance coefficient beyond the actual fiber saturation point.
3. In the desorption phase, loss of bound water begins at nearly 41% EMC. A region hence exists where the loss of bound water takes place in the presence of liquid water. The range of EMC of this region will depend on the size distribution of capillaries among wood species.

ACKNOWLEDGMENTS

The authors are grateful to Professor Yves Fortin for valuable suggestions and help. This research was supported by the National Council for Scientific and Technological Development of Brazil (CNPq) and the Natural Sciences and Engineering Research Council of Canada.

REFERENCES

BODIG, J., AND B. A. JAYNE. 1982. Mechanics of wood and wood composites. Van Nostrand Reinhold, New York, NY.

BROWN, H. P., A. J. PANSHIN, AND C. C. FORSAITH. 1949. Textbook of wood technology. Vol. I, McGraw-Hill Book Co. Inc., New York, NY.

CLOUTIER, A., AND Y. FORTIN. 1991. Moisture content-water potential relationship of wood from saturated to dry conditions. Wood Sci. Technol. 25:263–280.

FORTIN, Y. 1979. Moisture content-matric potential relationship and water flow properties of wood at high moisture contents. Ph.D. Thesis, University of British Columbia, Vancouver, BC, Canada.

GOULET, M. 1968. Phénomènes de second ordre de la sorption d'humidité dans le bois au terme d'un conditionnement de trois mois à température normale. Seconde partie: Essais du bois d'érable à sucre en compression radiale. Note de recherches N° 3, Département d'exploitation et utilisation des bois, Université Laval, Québec, Canada.

———, AND R. E. HERNÁNDEZ. 1991. Influence of moisture sorption on the strength of sugar maple wood in tangential tension. Wood Fiber Sci. 23(2):197–206.

GRIFFIN, D. M. 1977. Water potential and wood-decay fungi. Ann. Rev. Phytopathol. 15:319–329.

HART, C. A. 1984. Relative humidity, EMC, and collapse shrinkage in wood. Forest Prod. J. 34(11/12):45–54.

HERNÁNDEZ, R. E. 1983. Relations entre l'état de sorption et la résistance du bois d'érable à sucre en traction tangentielle. M.Sc. Thesis, Département d'exploitation et utilisation des bois, Université Laval, Québec, Canada.

———. 1993. Influence of moisture sorption on the compressive properties of hardwoods. Wood Fiber Sci. 25(1): 103–111.

———. 2005. Influence of extraneous substances, wood density and interlocked grain on the physical and mechanical properties of some tropical hardwoods. Part II: Fiber saturation point. Holzforschung (submitted).

———, AND M. BIZOŇ. 1994. Changes in shrinkage and tangential compression strength of sugar maple below and above the fiber saturation point. Wood Fiber Sci. 26(3):360–369.

KELSEY, K. E. 1956. The shrinkage intersection point–its significance and the method of its determination. Forest Prod. J. 6:411–416.

MENON, R. S., A. L. MACKAY, J. R. T. HALEY, M. BLOOM, A. E. BURGESS, AND J. S. SWANSON. 1987. An NMR determination of the physiological water distribution in wood during drying. J. Appl. Polym. Sci. 33:1141–1155.

NADERI, N., AND R. E. HERNÁNDEZ. 1997. Effect of a rewetting treatment on the dimensional changes of sugar maple wood. Wood Fiber Sci. 29(4):340–344.

PANSHIN, A. J., AND C. DE ZEEUW. 1980. Textbook of wood technology. 4th ed., McGraw-Hill, New York, NY.

ROBERTSON, A. A. 1965. Investigation of the cellulose-water relationship by the pressure plate method. Tappi 48(1): 568–573.

SIAU, J. F. 1984. Transport processes in wood. Springer-Verlag, New York, NY.

———. 1995. Wood: Influence of moisture on physical

properties. Virginia Polytechnic Institute and State University, Blacksburg, VA.

SKAAR, C. 1988. Wood-water relations. Springer-Verlag, New York, NY.

SLIKER, A. 1978. Strain as a function of stress, stress rate, and time at 90° to the grain in sugar pine. Wood Sci. 10(4):208–219.

STEVENS, W. C. 1963. The transverse shrinkage of wood. Forest Prod. J. 13(9):386–389.

STONE, J. E., AND A. M. SCALLAN. 1967. The effect of component removal upon the porous structure of the cell wall of wood. II. Swelling in water and the fiber saturation point. Tappi 50(10):496–501.

TIEMANN, H. D. 1906. Effect of moisture upon the strength and stiffness of wood. USDA Forest Service, Bulletin 70.

TREMBLAY, C., A. CLOUTIER, AND Y. FORTIN. 1996. Moisture content-water potential relationship of red pine sapwood above the fiber saturation point and determination of the effective pore size distribution. Wood Sci. Technol. 30: 361–371.

WHEELER, E. A. 1982. Ultrastructural characteristics of red maple (*Acer rubrum* L.) wood. Wood Fiber 14(1):43–53.

U.S. DEPARTMENT OF AGRICULTURE, FOREST SERVICE, FOREST PRODUCTS LABORATORY. 1974. Wood handbook: Wood as an engineering material. USDA Agric. Handb. 72. Rev. USDA, Washington, DC.